Preprint Title	Model compound met the key structural and spectroscopic features of [FeFe]-hydrogenase active site
Authors	Li Hai, Tianyong Zhang, Shuang Jiang, Xiaoyuan Ma, Di Wang and Bin Li
Publication Date	30 Okt 2019
Article Type	Full Research Paper
Supporting Information File 1	SI.docx; 799.2 KB
ORCID® iDs	Bin Li - https://orcid.org/0000-0002-8509-9833

Model compound met the key structural and spectroscopic features of [FeFe]-hydrogenase active site

*Li Hai,[a] Tianyong Zhang,[*a, b, c] Shuang Jiang,[*a] Xiaoyuan Ma,[a] Di Wang,[a] and Bin Li,[*a, c]*

[a] Tianjin Key Laboratory of Applied Catalysis Science and Technology, School of Chemical Engineering and Technology, Tianjin University, Tianjin 300354, China.

[b] Collaborative Innovation Center of Chemical Science and Engineering (Tianjin), Tianjin 300072, China

[c] Tianjin Engineering Research Center of Functional Fine Chemicals, Tianjin 300354, China

ABSTRACT Biomimetic synthesis of the [FeFe]-hydrogenase active site draws considerable attention of scientists for its amazing catalytic efficiency on reversible transition between proton and hydrogen. $Fe_2(CO)_3[\mu\text{-}(SCH(CH_2CH_3)CH_2S)](\mu\text{-DPPM})(\kappa^1\text{-DPPM})$ (compound **1**) which replicated key structural aspects of the natural [FeFe]-hydrogenase was designed and synthesized. **1** showed that the wavenumbers in IR were close to those of the natural [FeFe]-hydrogenase active site. In addition, **1** achieved the low oxidation potentials at -0.48 V and -0.26 V, respectively. In the assistance of ethyl located in the S-S bridging structure, the asymmetrical substitution with sterically encumbering and electron-rich ligands in **1** may offer a thorough protection for forming and stabilizing the open site in the rotated structure.

KEYWORDS [FeFe]-hydrogenase; Structure simulation; Model compound; Enzymes; Oxidation potential

INTRODUCTION

With an increasing concern of global energy crisis and the damage to the environment, it is an urgency to find the non-fossil energy resources which can support the sustainable development of human society. Hydrogen production is one of most promising technologies since hydrogen is a high effective and green energy carrier. Scientists achieved lots of progresses on science and technology inspired by the Nature. Hydrogenases, the enzymes which can be found in the anaerobic microorganism, can reversibly catalyze the transition between proton and hydrogen molecule with amazing efficiency.[1-3] After determination of the crystal structure of [FeFe]-hydrogenase two decades ago,[4-6] chemists put a lot of efforts on trying to biomimetic synthesize the [FeFe]-hydrogenase active site for it may offer a promising solution to generating hydrogen and show a potential to apply in hydrogen fuel cells.[7,8]

Natural [FeFe]-hydrogenases active sites have common features including three CO, three electron-rich ligands and a dithiolate that bridges di-iron (Scheme 1). Numerous organometallic complexes which can be expressed as $Fe_2(CO)_xL_{6-x}(\mu\text{-SXS})$ (X=R, N or O) were synthesized to explore the possibilities to simulate the structural and/or functional features of [FeFe]-hydrogenase.[9-13] However, the complicated biological groups and steric inhibition in the natural [FeFe]-hydrogenase make it a challenge for researchers to reproduce. What's more, the sensitivity to oxygen and various other factors render it more difficult to study the model compound of [FeFe]-hydrogenase active site. So far, model compounds which could achieve the structure with three electron-rich substitution ligands, three CO and the spectroscopic

2

resemblance to active site of the natural [FeFe]-hydrogenase have been rare [14,15]. Therefore, it remains a salient goal for researchers to synthesize the appropriate structure in the Fe^IFe^I redox level, a cornerstone for further study of the mechanism of hydrogen production and oxidation process.

The pioneers in this area, such as Darensbourg's group，Rauchfuss's group and Pickett's group, have given guidance for the synthesis of the appropriate Fe^IFe^I precursors: 1) Asymmetric coordination of two Fe^I centres to allow different valent state in the redox process, 2) Good electron-donating ligands and 3) Sterically encumbering ligands to stabilize the Fe^{II} and protect the open site formed when one Fe is inverted with respect to the other, which is also known as "rotated state". In rotated state, a semi-bridging carbonyl is located between two Fe centres and open site could bond with proton, H_2 or CO.[16-18] Generally speaking, there are two methods to achieve above restricted conditions: The first is using μ_2-SRS or $(\mu$-SR$)_2$ bridging structure with bulk effect;[10,19] Second, asymmetrically substituting CO with appropriate steric hindrance ligand(s). In consideration of benign electron-donating performance, flexible substitution methods and selectable bulk structures, phosphorus ligands were extensively employed as substitution group in the model compounds of [FeFe]-hydrogenase.[20,21] Taking a classic model compound as an example, $(\mu$-dmpdt$)[Fe(CO)_2PMe_3]_2$ (dmpdt = 2,2-dimethyl-1,3-propanedithiolate) was given by Darensbourg's group and the study showed that the formation of open site was oriented by the twisting direction of dimethyl seated on the dithiolate bridging structure while PMe_3 groups were in the symmetrical position on the each side of Fe center.[22]

In this work, we designed and prepared $Fe_2(CO)_3[\mu$-(SCH(CH$_2$CH$_3$)CH$_2$S)]$(\mu$-DPPM$)(\kappa^1$-DPPM) {**1**, DPPM= bis-(diphenylphosphino) methane} with three CO and a dithiolate bridging structure, which showed a similar secondary coordination structure with the natural [FeFe]-

hydrogenase active site. More importantly, **1** met all the aforementioned three requirements (Scheme 1). **1** showed low wavenumbers in IR which were closer to the natural [FeFe]-hydrogenase. The oxidation potential of **1** showed in CV test also indicated its resemblance to the electronic feature of [FeFe]-hydrogenase. In addition, the substitution ligands DPPM in **1** had great steric hindrance (molecular weight 1085 with 8 benzene rings), making it a potential candidate for further study on the mechanism of hydrogen production and oxidation [23, 24]. As a comparative compound, $Fe_2(CO)_5[\mu-(SCH(CH_2CH_3)CH_2S)]$ (κ^1-DPPM) (**2**) was also studied by IR, UV-vis, X-ray single crystal diffraction and CV to elucidate the effects of μ-DPPM ligand on **1**.
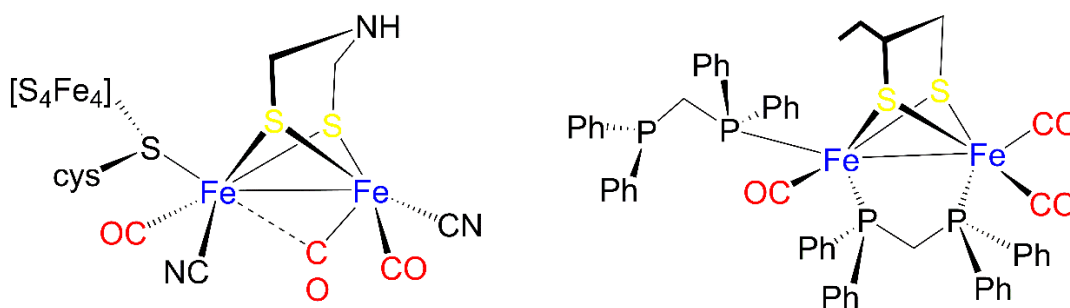
Scheme 1. The rotated structure of active site of [FeFe]-hydrogenase (left) and the present compound **1** (right)

RESULTS AND DISCUSSION

Structure analysis

IR results of **1-3** (**3**, $Fe_2(CO)_6[\mu-(SCH(CH_2CH_3)CH_2S)]$) in ν(CO) region were depicted in Figure 1. Overall, compared with **3,** the wavenumbers of **1** and **2** were all shifted to the lower position. Meanwhile, the wavenumbers of **1** were much lower than those of **2**. To be specific, the highest absorption peaks of **1** (1959(s)) and **2** (2044(s)) shifted to lower wavenumbers by 114

cm^{-1} and 29 cm^{-1} in comparison with 2073 cm^{-1} of **3**, respectively. Moreover, for the lowest absorption peaks, there were 120 cm^{-1} and 62 cm^{-1} negative-shifts in **1** and **2** compared with the corresponding peak of **3**, respectively. The lower wavenumbers in IR of **1** were due to the enhanced electron density around Fe^{I} centers by μ-DPPM. On the other hand, the similar substitution method to the natural [FeFe]-hydrogenase active site made **1** an achievement of a closer replication of IR features of natural [FeFe]-hydrogenase (1967(w), 1943(s), 1907(m), 1877(m)), which indicated a step forward to simulate the structure of [FeFe]-hydrogenase active site. [25]
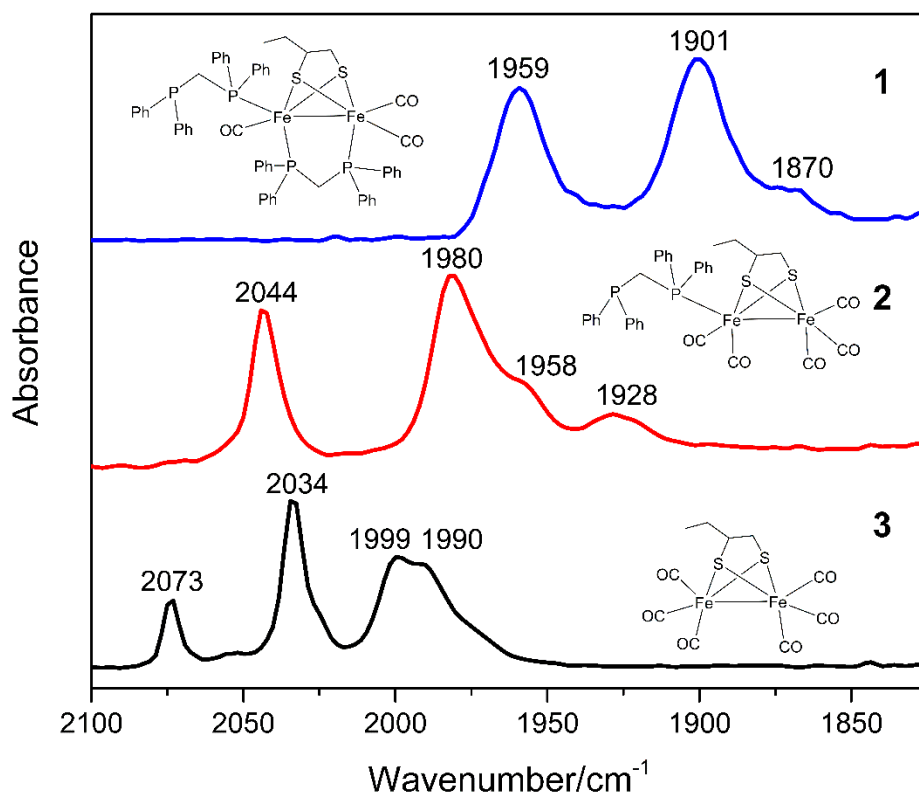

Figure 1. The IR spectra of **1-3** in CH$_2$Cl$_2$

To further investigate the influence of the μ-DPPM ligand on spectroscopic effect, UV-vis of **1-3** in CH$_2$Cl$_2$/ *n*-hexane (v/v, 2:8) were measured (Figure 2). Each compound showed two

main characteristic peaks in UV-vis. The absorption peaks around 235 nm of **1** and **2** were assigned as the sum of K band of π-π* transition in benzene rings and n-δ* transition in auxochrome SRS group. The absorption peaks in 320-390 nm were assigned as n-π* transition in CO group. Because of the coordination of more PPh$_2$ units to Fe centres, which increases the electron density around Fe and also introduces the changes of electron environment to CO and other ligands, the wavelengths of **1** were red-shifted compared with **2** and **3**, which was a mirror to reflect IR analysis. The variation of absorption intensity in 320-390 nm may be caused by the steric hindrance effect. **1** and **2** were able to absorb visible light to some extent and there was no absorbance in the range from 600 nm to 800 nm in all four tested compounds (**1-3** and DPPM).
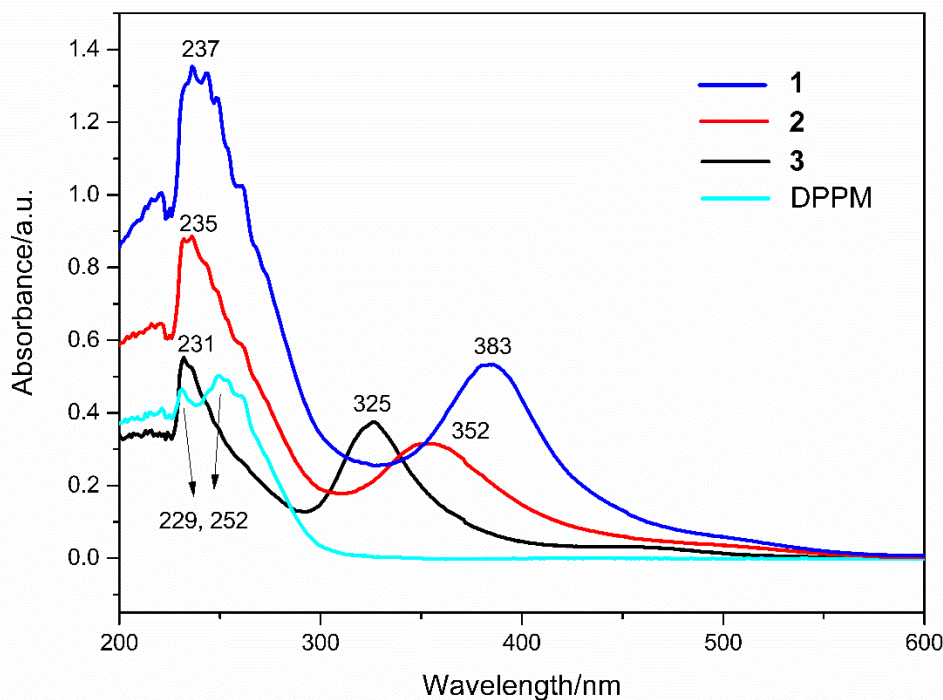

Figure 2. The UV-vis spectra of **1-3** and DPPM

Single crystals of **1** and **2** were obtained by slow evaporation at 0 ºC from CH$_2$Cl$_2$/n-hexane solution. Crystal data and structure refinement of **1** and **2** were listed in Table S1. Molecular

structures of **1** and **2** were exhibited in Figure 3. [26] μ-DPPM and κ[1]-DPPM mimicked CN^{-} and [4Fe-4S] cluster in **1**, respectively. To fully expand the ligands and reduce steric hindrance, the Fe-Fe distance of **1** (2.51 (9) Å) was slightly longer than that in **2** (2.50 (9) Å), so did the average distances of Fe-S, which is 2.26 Å compared to 2.25 Å. The average bond angle centred on Fe in basal position of **1** (97.5 deg.) was 3.0 deg. smaller than that of **2** (100.5 deg.), which leaving C(2) and P(3) in axial position more space to expand. As we can see, the bond angles of C(2)-Fe(1)-Fe(2) [157.4 (16) deg.] and P(3)-Fe(2)-Fe(1) [156.7 (5) deg.] in **1** were approximately 6 deg. greater than that of C(1)-Fe(1)-Fe(2) [150.8 (15) deg.] and P(1)- Fe(2)-Fe(1) [151.6 (4) deg.] in corresponding positions of **2**, respectively. In addition, the Fe-P (μ-DPPM) distance (average 2.20 Å) in **1** was shorter than Fe-P (κ-DPPM) (2.22 Å).
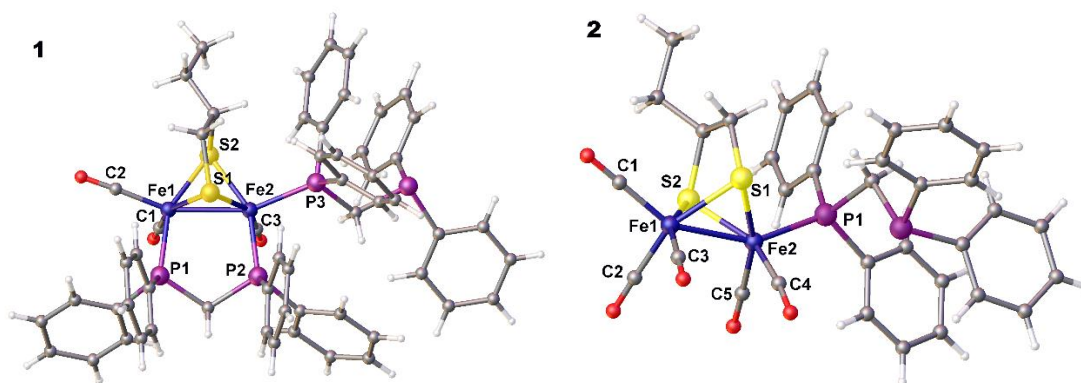

Figure 3. Molecular structures of **1** and **2**. Selected bond lengths [Å] and angles [deg] for **1**: Fe(1)-C(1) 1.77(6), Fe(1)-C(2) 1.78(7), Fe(1)-P(1) 2.20 (18), Fe(1)-Fe(2) 2.51 (11), Fe(2)-C(3) 1.75(6), Fe(2)-P(2) 2.20 (17), Fe(2)-P(3) 2.22 (15), C(1)-Fe(1)-Fe(2) 97.9 (19), C(2)-Fe(1)-Fe(2) 157.4 (2), P(1)-Fe(1)-Fe(2) 96.9 (6), C(3)-Fe(2)-Fe(1) 98.5 (18), P(2)-Fe(2)-Fe(1) 96.7 (5), P(3)-Fe(2)-Fe(1) 156.7 (6). Selected bond lengths [Å] and angles [deg] for **2:** Fe(1)-C(3) 1.78 (6), Fe(1)-C(1) 1.79 (5), Fe(1)-C(2) 1.80 (7), Fe(1)-Fe(2) 2.50 (9), Fe(2)-C(4) 1.77 (4), Fe(2)-C(5) 1.77 (5), Fe(2)-P(1) 2.22 (11), C(3)-Fe(1)-Fe(2) 102.3 (16), C(1)-Fe(1)-Fe(2) 150.8 (15), C(2)-Fe(1)-Fe(2) 97.9 (16), C(4)-Fe(2)-Fe(1) 96.4 (12), C(5)-Fe(2)-Fe(1) 105.6 (13), P(1)-Fe(2)-Fe(1) 151.6 (4)

During the process of hydrogen evolution as well as its oxidation, the key is the formation of the open site on Fe center where H^+ or H_2 can bond. Basing on experimental results and DFT calculations,[22,27,28] the Fe center in the rotated structure of model compound of [FeFe]-hydrogenase active site should be formed and stabilized under the protection of electron-rich ligand(s) with bulk effect. In the proposed rotated structure of **1,** as shown in Figure 4, the open site could be formed on the side of $Fe(CO)(\kappa^1\text{-DPPM})$ so that it can take the advantage of protection from fully expanded benzene rings of PPh_2, which looks like the butterfly with open wings. The Fe center can be stabilized under "the wings of butterfly" where located more electron donating ligands with bulk effect. Furthermore, ethyl located in the S-S bridging moiety can also make a contribution to stabilize the rotated structure by increasing the steric effect to some extent. A shelter formed under the guard of PPh_2 and ethyl offers a good protection for the open site.
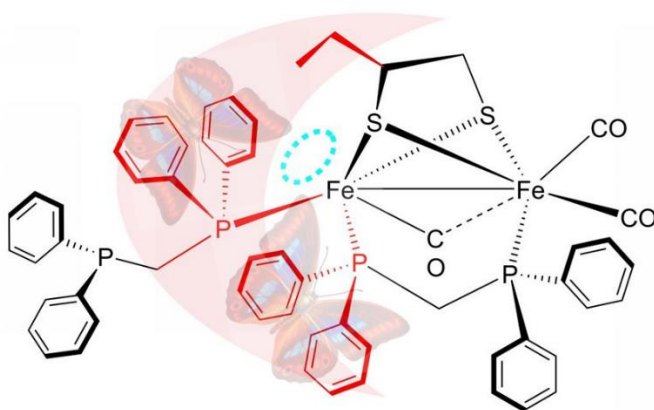

Figure 4. Proposed rotated structure of **1**. PPh_2 groups and ethyl located in the S-S bridging moiety can protect the open site which is shown as a blue circle.

Electrochemical properties

The cyclic voltammograms (CVs) of **1** were conducted under N_2 and CO, respectively. Figure 5a showed that a new peak appeared at -0.45 V when CV test carried out under CO atmosphere. In the meantime, the reduction part experienced a shift towards positive direction. The variation of CV conducted under different atmosphere indicated that μ-DPPM did not inhibit the formation of open site which showed in the Figure 4. The specific mechanism of the difference performance of CV test under CO atmosphere comparing with N_2 atmosphere was shown in Figure 5b.[28,29] The rotated state of **1** formed under CO atmosphere allowed the occupation of CO at the open site, which made a contribution to the stability of Fe^IFe^{II} so that we can observe the peak located at -0.45 V.[30,31] Reorganisation of steric arrangements and electronic effect may slightly reduce the electron density around Fe centres, so that the reduction peaks of **1** went through a positive shift by 0.06 V and 0.09 V, respectively. The same phenomenon can be observed when CV was conducted in CH_2Cl_2 solution. While in N_2 atmosphere without CO occupying the open site, the oxidation process went through two-electron transition. assistance of ethyl located in the S-S bridging moiety may also stabilize the oxidation state of **1**. Figure S1 showed CVs of **2** in different atmosphere.

In the CV of **1**, ΔE_p^1 ($E_{1/2}^1$ = -0.48 V) and ΔE_p^2 ($E_{1/2}^2$ = -0.26 V) were all approximately 60 mV, respectively, which suggested that the two oxidation events were reversible.[32] The CV of **2** did not show the reversible oxidation characteristic of **1** (Fig. S1), which indicates the striking significance of the bridging ligand μ-DPPM. The irreversible reduction peaks of **1** were at -2.28 V and -2.43 V, compared with reduction peaks at -1.94 V and -2.31 V of **2**. The distinction between **1** and **2** in the reduction potentials was also an echo of the IR and UV-vis that **1** was more electron-rich, leading to more negative reductive potential.
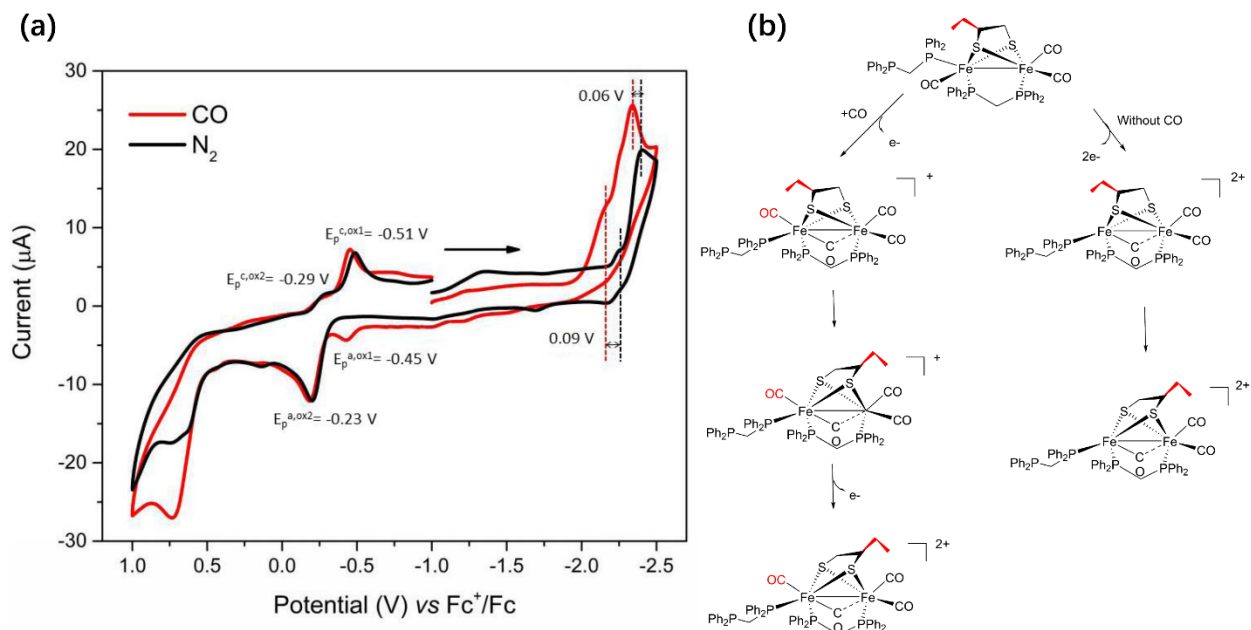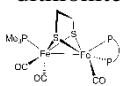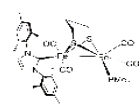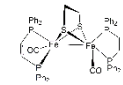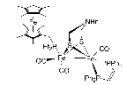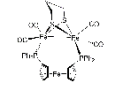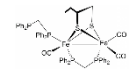
Figure 5. Comparisons of CVs of **1** at 50 mV/s (a) and proposed mechanism of **1** oxidation under CO and N₂(b).

Because of hard-to-reach conditions for synthesis of the appropriate Fe^IFe^I precursors which can serve in mechanism study, so far, the reported complexes which can meet aforementioned requirements have been rare. Table 1 listed structures, IR and oxidation potential data of the classic mixed valence models of [FeFe]-hydrogenase active site. In the structure of natural [FeFe]-hydrogenase, there are three CO and three substituent groups, which is the first challenge to mimic due to prominent steric effect. On the other hand, favorable electronic effect offered by μ-DPPM and $κ^1$-DPPM made ν(CO) in IR of **1** show most similarities to natural [FeFe]-hydrogenase. One step further, oxidation potentials of **1** in CV test were also competitive compared with compounds listed. Above all, **1** showed a good potential to serve as a model of

[FeFe]-hydrogenase active site not only in the structural feature but also in the spectroscopic as well as electronic aspects.

Table 1. Comparisons of models of [FeFe]-hydrogenase active site for mixed valence study

Compounds	IR ν(CO)/cm^{-1}	Oxidation potential/V (vs Fc$^+$/Fc)	Ref.
CaHydF Reduced with dithionite	1967(w), 1943(s), 1907(m), 1877(m)	-0.45	25, 33
	1943, 1892		14
	1972 (s), 1933 (vs), 1897 (s), 1882 (sh)	-0.47 (Fe^{I}Fe^I / Fe^{I}Fe^{II}) 0.14 (Fe^{I}Fe^{II}/Fe^{II}Fe^{II})	34
	1888(s), 1868(s)	-0.17 (Fe^{I}Fe^I / Fe^{I}Fe^{II}) 0.60 (Fe^{I}Fe^{II}/Fe^{II}Fe^{II})	35
	2022(w), 1958(s), 1945(m), 1907 (s), 1897(s), 1881 (m)		15
	1986(s), 1949(vs), 1918(s), 1896(w)	0.05 (Fe centers) 0.685 (ferrocene moiety)	36
	1959(s), 1901(s), 1870(w)	-0.48 (Fe^{I}Fe^I / Fe^{I}Fe^{II}) -0.26 (Fe^{I}Fe^{II}/Fe^{II}Fe^{II})	Our work

IR of models were in the CH$_2$Cl$_2$ solution. CVs were conducted in the CH$_3$CN.

CONCLUSIONS

In summary, Fe$_2$(CO)$_3$[μ-(SCH(CH$_2$CH$_3$)CH$_2$S)](μ-DPPM)(κ^1-DPPM) (**1**) and its contrastive compound Fe$_2$(CO)$_5$[μ-(SCH(CH$_2$CH$_3$)CH$_2$S)] (κ^1-DPPM) (**2**) were synthesized and fully characterized by IR, UV and X-ray single crystal diffraction. Wavenumbers in IR and oxidation potentials in CV of **1** were quite close to the natural [FeFe]-hydrogenase active site. Asymmetrical substitution with bulk steric effect made **1** meet the key requirements to secondary coordination structure of the natural [FeFe]-hydrogenase active site, which achieved a further

progress on the structural simulation. With the shelter of the "butterfly shape" ligands (which refers to PPh$_2$) as well as assistance of ethyl located in the S-S bridging moiety, open site may get better protection. In addition, **1** shows comparable structural, spectroscopic as well as electronic features of [FeFe]-hydrogenase active site compared with the reported classic model compounds. We cautiously draw a conclusion that **1** can be a good candidate for the further study of [FeFe]-hydrogenase, which may give us a chance to further reveal the catalytic mechanism of natural [FeFe]-hydrogenase. In the future work, we may focus on replacing inert ligand with non-innocent ligand to mimic the [4Fe-4S] cluster of [FeFe]-hydrogenase active site to try to get the model compound with more similar structure as well as better performance.

EXPERIMENTAL SECTION

General procedures

All synthetic operations were conducted under N$_2$ atmosphere using Schlenk line techniques. All materials were available commercially and used as received.

The NMR spectra were recorded with a Bruker AVANCE III 400MHz NMR spectrometer. The IR were measured on a Shimadzu FTIR- 8400 spectrometer. Heraeus CHN-Rapid was used for elemental analysis. The UV-vis spectra were determined by the UV-vis diffuse reflectance spectrum (UV-3600). X-ray single crystal diffraction data were recorded with a Rigaku MM-007 (rotating anode) diffractometer. Data were collected by using a graphite monochromator with Mo-Kα radiation (λ = 0.71073 Å) in the ω-ϕ scanning mode. Data collection, reduction, and absorption correction were performed by CRYSTALCLEAR. The structure was solved by direct methods using SHELXS.

Electrochemical studies were performed on a CHI760D electrochemical work station at room temperature (25 °C) with a three-electrode system. A glassy carbon electrode (diameter 3 mm) was the working electrode, a saturated Ag/AgNO₃ electrode was the reference electrode, and a platinum wire was the auxiliary electrode. The potentials were calibrated using ferrocene as an internal standard substance. Controlled potential coulometry in CH_3CN was conducted using an air-tight glass double compartment cell. The working compartment was fitted with a platinum plate electrode (1×1 cm) and an Ag/AgCl electrode. The auxiliary compartment was fitted with a platinum wire electrode.

Synthesis of compound 1

μ-(SCH(CH₂CH₃)CH₂S)-Fe₂(CO)₆ (400 mg, 1.0 mmol) and Me₃NO (75 mg, 1.0 mmol) were dissolved in toluene (5 mL) and the solution was kept stirring at room temperature until its colour turned brownish black. Then DPPM (769 mg, 2.0 mmol) was added to the solution. The mixture was stirred for 5 h at 110 °C. Toluene was removed in *vacuo*. Separation and purification of reaction products were conducted by a neutral alumina column and gradient eluted with CH₂Cl₂/ n-hexane (0/10, 1/9, 2/8, v/v). The fourth band with red colour was gathered as target substance which was air-stable. Yield: 342.9 mg (31.6%). IR (CH₂Cl₂, cm⁻¹): ν(CO) 1959(s), 1901(s), 1870(w). UV-Vis (CH₂Cl₂/ *n*-hexane, v/v=2/8): λ_{max} (ε)=237 nm (ε=11000 L*mol⁻¹*cm⁻¹), 383 nm (ε=4347 L*mol⁻¹*cm⁻¹); Elemental analysis (%) calculated for C₅₇H₅₂Fe₂O₃P₄S₂ (found): C 63.10 (62.91); H 4.80 (4.85); S 5.90 (5.83). ¹³C NMR (100 MHz, CDCl₃): δ 133.77 (s, Ph), 133.67 (s, Ph), 133.00-132.38 (m, Ph), 132.25-132.05 (m, Ph), 131.86 (s, Ph), 131.76 (s, Ph), 131.05-130.75 (m, Ph), 129.20-128.69 (m, Ph), 128.30-127.93 (m, Ph), 127.64-126.93 (m, Ph), 61.33 (s, CH₂(S)***C***H(S)CH₂CH₃), 54.75-54.58 (m, ***C***H₂(S)CH(S)CH₂CH₃), 53.43 (s, CH₂(S)CH(S)***C***H₂CH₃), 29.42-29.32 (m, PCP), 14.07 (s, CH₂(S)CH(S)CH₂***C***H₃). ³¹P NMR (162

MHz, CDCl$_3$): δ 57.35-56.62 (m, 1P), 54.42-53.94 (m, 1P), -26.58-(-26.97) (m, 1P), -49.99 (s, 1P). ^{1}H NMR (400 MHz, CDCl$_3$): δ 7.59-7.02 (m, Ph), 6.96 (t, J=8.4 Hz, Ph), 6.78 (t, J=6.4 Hz, Ph), 5.33 (s, H-P), 4.09 (q, J=10.8, 6.4 Hz), 3.39 (q, J=12.8, 11.2 Hz, CH$_2$(S)C**H**(S)CH$_2$CH$_3$), 3.03 (d, J=15.6 Hz, C**H**$_2$(S)CH(S)CH$_2$CH$_3$), 2.51-2.40 (m, CH$_2$(S)CH(S)C**H**$_2$CH$_3$), 1.66-1.52 (m, PC**H**$_2$P), 1.45-1.28 (m, PC**H**$_2$P), 0.81 (t, J=6.8 Hz, CH$_2$(S)CH(S)CH$_2$C**H**$_3$).

Synthesis of compound 2

The procedure used to prepare compound **2** was similar with the operations above except that DPPM (384 mg, 1.0 mmol) was employed and the second band eluted in the neutral alumina column was collected. Yield: 288.8 mg (38.2%). IR (CH$_2$Cl$_2$, cm^{-1}): ν(CO) 2044(s), 1980(s), 1958(w), 1928(w). UV-Vis (CH$_2$Cl$_2$/ *n*-hexane, v/v=2/8): λ$_{max}$ (ε)=235 nm (ε=7189 L*mol^{-1}*cm^{-1}), 352 nm (ε=2563 L*mol^{-1}*cm^{-1}); Elemental analysis (%) calculated for C$_{34}$H$_{30}$Fe$_2$O$_5$P$_2$S$_2$ (found): C 53.97 (54.06); H 3.97 (3.90); S 8.46 (8.33). ^{13}C NMR (100 MHz, CDCl$_3$): δ 215.32, (m, CO), 210.43 (m, CO), 133.30-132.16 (m, C, Ph), 130.21 (d, J=2.0 Hz, 2C, Ph), 130.06 (d, J=1.9 Hz, 2C, Ph), 128.72-125.09 (m, C, Ph), 54.43 (d, J=3 Hz, CH$_2$(S)**C**H(S)CH$_2$CH$_3$), 40.84 (d, J=2.5 Hz, **C**H$_2$(S)CH(S)CH$_2$CH$_3$), 29.67 (s, 2C, CH$_2$(S)CH(S)**C**H$_2$CH$_3$ and PCP), 14.04 (s, CH$_2$(S)CH(S)CH$_2$**C**H$_3$). ^{31}P NMR (162 MHz, CD$_2$Cl$_2$): δ 55.49-54.57 (m), -25.50- (-26.32) (m). ^{1}H NMR (400 MHz, CDCl$_3$): δ 7.61 (dq, J=25.6, 15.2, 2.8 Hz, Ph), 7.36-7.18 (m, Ph), 3.30 (dd, J=8.4, 2.0 Hz, CH$_2$(S)C**H**(S)CH$_2$CH$_3$), 1.70 (d, J=2 Hz, C**H**$_2$(S)CH(S)CH$_2$CH$_3$), 1.36 (hex, J=15.6, 8.4, 7.6 Hz, CH$_2$(S)CH(S)C**H**$_2$CH$_3$), 0.93 (J=13.2, 6.4 Hz, PC**H**$_2$P), 0.82 (t, J=7.2 Hz, CH$_2$(S)CH(S)CH$_2$C**H**$_3$).

AUTHOR INFORMATION

Corresponding Author

*Email: libin@tju.edu.cn; tyzhang@tju.edu.cn; shuangjiang@tju.edu.cn.

Notes

There are no conflicts to declare.

References

(1) Glick, B. R.; Martin, W. G.; Martin, S. M. Purification and properties of the periplasmic hydrogenase from Desulfovibrio desulfuricans. Can. J. Microbiol., 1980, 26, 1214-1223.

(2) Hatchikian, E. C.; Magro, V.; Forget, N.; Nicolet, Y.; FontecillaCamps, J. C. Carboxy-terminal processing of the large subunit of [Fe] hydrogenase from desulfovibrio desulfuricans ATCC 7757. J. Bacteriol., 1999, 181, 2947-2952.

(3) Fourmond, V.; Greco, C.; Sybirna, K.; Baffert, C.; Wang, P. H.; Ezanno, P.; Montefiori, M.; Bruschi, M.; Meynial-Salles, I.; Soucaille, P.; Blumberger, J.; Bottin, H.; Gioia, L. D.; Leger, C. The oxidative inactivation of FeFe hydrogenase reveals the flexibility of the H-cluster. Nat. Chem., 2014, 6, 336-342.

(4) Peters, J. W.; Lanzilotta, W. N.; Lemon, B. J.; Seefeldt, L. C. X-ray crystal structure of the Fe-only hydrogenase (CpI) from clostridium pasteurianum to 1.8 angstrom resolution. Science, 1998, 282, 1853-1858.

(5) Nicolet, Y.; Piras, C.; Legrand, P.; Hatchikian, C. E.; Fontecilla-Camps, J. C. Desulfovibrio desulfuricans iron hydrogenase: The structure shows unusual coordination to an active site Fe binuclear center. Structure, 1999, 7, 13-23.

(6) Pandey, A. S.; Harris, T. V.; Giles, L. J.; Peters, J. W.; Szilagyi, R. K. Dithiomethylether as a ligand in the hydrogenase H-cluster. J. Am. Chem. Soc., 2008, 130, 4533-4540.

(7) Wang, N.; Wang, M.; Chena, L.; Sun, L. C. Reactions of [FeFe]-hydrogenase models involving the formation of hydrides related to proton reduction and hydrogen oxidation. Dalton Trans., 2013, 42, 12059-12071.

(8) DuBois, D. L.; Bullock, R. M. Molecular electrocatalysts for the oxidation of hydrogen and the production of hydrogen - The role of pendant amines as proton relays. Eur. J. Inorg. Chem., 2011, 7, 1017-1027.

(9) Cheng, M. L.; Wang, M.; Zheng, D. H.; Sun, L. C. Effect of the S-to-S bridge on the redox properties and H_2 activation performance of diiron complexes related to the [FeFe]-hydrogenase active site. Dalton Trans., 2016, 45, 17687-17696.

(10) Razavet, M.; Borg, S. J.; George, S. J.; Best, S. P.; Fairhursta, S. A.; Pickett, C. J. Transient FTIR spectroelectrochemical and stopped-flow detection of a mixed valence {Fe(I)–Fe(II)} bridging carbonyl intermediate with structural elements and spectroscopic characteristics of the di-iron sub-site of all-iron hydrogenase. Chem. Commun., 2002, 7, 700-701.

(11) Winkler, M.; Senger, M.; Duan, J.; Esselborn, J.; Wittkamp, F.; Hofmann, E.; Apfel, U-P.; Stripp, S. T.; Happe, T. Accumulating the hydride state in the catalytic cycle of [FeFe]-hydrogenases Nat. Commun., 2017, 16115, 1-7.

(12) Simmons, T. R.; Berggren, G.; Bacchi, M.; Fontecave, M.; Artero, V. Mimicking hydrogenases: From biomimetics to artificial enzymes. Coordin. Chem. Rev., 2014, 270–271, 127-150.

(13) Tard, C.; Pickett, C. J. Structural and functional analogues of the active sites of the [Fe]-, [NiFe]-, and [FeFe]-hydrogenases. Chem. Rev., 2009, 109, 2245-2274.

(14) Justice, A. K.; Zampella, G.; Gioia, L. D.; Rauchfuss, T. B.; Vlugt, J. I. V.; Wilson, S. R. Chelate control of diiron(I) dithiolates relevant to the [Fe−Fe]-hydrogenase active site. Inorg. Chem., 2007, 46, 1655-1664.

(15) Camara, J. M.; Rauchfuss, T. B. Combining acid-base, redox and substrate binding functionalities to give a complete model for the [FeFe]-hydrogenase. Nat. Chem., 2012, 4, 26-30.

(16) Thomas, C. M.; Liu, T. B.; Hall, M. B.; Darensbourg, M. Y. Series of mixed valent Fe(II)Fe(I) complexes that model the H_{ox} state of [FeFe] hydrogenase: Redox properties, density-functional theory investigation, and reactivities with extrinsic CO. Inorg. Chem., 2008, 47, 7009-7024.

(17) Hsieh, C. H.; Erdem, Ö. F.; Harman, S. D.; Singleton, M. L.; Lubitz, W.; Popescu, C. V.; Reibenspies, J. H.; Brothers, S. M.; Hall, M. B.; Darensbourg, M. Y. Structural and spectroscopic features of mixed valent $Fe^{II}Fe^{I}$ complexes and factors related to the rotated configuration of diiron hydrogenase. J. Am. Chem. Soc., 2012, 134, 13089-13102.

(18) Sommer, C.; Adamska-Venkatesh, A.; Pawlak, K.; Birrell, J. A.; Rüdiger, O.; Reijerse, E. J.; Lubitz, W. Proton coupled electronic rearrangement within the H- cluster as an essential step in the catalytic cycle of [FeFe] hydrogenases. J. Am. Chem. Soc., 2017, 139, 1440-1443.

(19) Zheng, D. H.; Wang, M.; Chen, L.; Wang, N.; Cheng, M. L.; Sun, L. C. The influence of a S-to-S bridge in diiron dithiolate models on the oxidation reaction: A mimic of the H^{air}_{ox} state of [FeFe]-hydrogenases. Chem. Commun., 2014, 50, 9255-9258.

(20) Li, R. X.; Liu, X. F.; Liu, T.; Yin, Y. B.; Zhou, Y.; Mei, S. K.; Yan, J. Electrocatalytic properties of [FeFe]-hydrogenases models and visible-light-driven hydrogen evolution efficiency promotion with porphyrin functionalized graphene nanocomposite. Electrochim. Acta, 2017, 237, 207-216.

(21) Carroll, M. E.; Chen, J.; Gray, D. E.; Lansing, J. C.; Rauchfuss, T. B.; Schilter, D.; Volkers, P. I.; Wilson, S. R. Ferrous carbonyl dithiolates as precursors to FeFe, FeCo, and FeMn carbonyl dithiolates. Organometallics, 2014, 33, 858-867.

(22) Singleton, M. L.; Bhuvanesh, N.; Reibenspies J. H.; Darensbourg M. Y. Synthetic support of De Novo design: Sterically bulky [FeFe]-hydrogenase models. Angew. Chem. Int. Ed., 2008, 47, 9492-9495.

(23) Justice, A. K.; Rauchfuss, T. B.; Wilson, S. R. Unsaturated, mixed-valence diiron dithiolate model for the H_{ox} state of the [FeFe] hydrogenase. Angew. Chem. Int. Ed., 2007, 46, 6152-6154.

(24) Schilter, D.; Camara, J. M.; Huynh, M. T.; Hammes-Schiffer, S.; Rauchfuss, T. B. Hydrogenase enzymes and their synthetic models: The role of metal hydrides. Chem. Rev., 2016, 116, 8693-8749.

(25) Czech, I.; Silakov, A.; Lubitz W.; Happe, T. The [FeFe]-hydrogenase maturase HydF from clostridium acetobutylicum contains a CO and CN− ligated iron cofactor. FEBS Lett., 2010, 584, 638-642.

(26) CCDC-1813061 and CCDC-1813060 contain the supplementary crystallographic data for 1 and 2, which can be obtained from The Cambridge Crystallographic Data Centre via www. ccdc.cam.ac.uk/data_request/cif.

(27) Thomas, C. M.; Darensbourg, M. Y.; Hall, M. B. Computational definition of a mixed valent Fe(II)Fe(I) model of the [FeFe]hydrogenase active site resting state. J. Inorg. Biochem., 2007, 101, 1752-1757.

(28) Arrigoni, F.; Bouh, S. M.; Gioia, L. D.; Elleouet, C.; Petillon, F. Y.; Schollhammer, P.; Zampella, G. Influence of the dithiolate bridge on the oxidative processes of diiron models related to the active site of [FeFe] hydrogenases. Chem. Eur. J., 2017, 23, 4364-4372.

(29) Hai, L.; Zhang, T. Y.; Zhang, X.; Zhang, G. H.; Li, B.; Jiang, S.; Ma, X. Y. Reversible isomerization of a novel [FeFe]- hydrogenase model complex and water-promoted electrocatalytic proton reduction. Electrochem. Commun., 2017, 82, 66-70.

(30) Chouffai, D.; Zampella, G.; Capon, J. F.; Gioia, L. D.; Goff, A. L.; Petillon, F. Y.; Schollhammer, P.; Talarmin, J. Electrochemical and theoretical studies of the impact of the chelating ligand on the reactivity of $[Fe_2(CO)_4(\kappa^2\text{-LL})(\mu\text{-pdt})]^+$ complexes with different

substrates (LL = I_{Me}-CH_2-I_{Me}, dppe; I_{Me} = 1-Methylimidazol-2-ylidene). Organometallics, 2012, 31, 1082-1091.

(31) Thomas, C. M.; Liu, T.; Hall, M. B.; Darensbourg, M. Y. Regioselective ^{12}CO/^{13}CO exchange activity of a mixed-valent Fe(II)Fe(I) model of the H_{ox} state of [FeFe]-hydrogenase. Chem. Commun., 2008, 13,1563–1565.

(32) $E_{1/2}$ is ($E^{a, ox}$ + $E^{c, ox}$)/2, ΔE_p is absolute difference value of $E^{a,ox}$ - $E^{c, ox}$.

(33) Schut, G. J.; Adams, M. W. W. The iron-hydrogenase of thermotoga maritima utilizes ferredoxin and NADH synergistically: A new perspective on anaerobic hydrogen production. J. Bacteriol., 2009, 191, 4451-4457.

(34) Liu, T.; Darensbourg, M. Y. A mixed-valent, Fe(II)Fe(I), diiron complex reproduces the unique rotated state of the [FeFe]hydrogenase active site. J. Am. Chem. Soc., 2007, 129, 7008-7009.

(35) Justice, A. K.; Nilges, M. J.; Rauchfuss, T. B.; Wilson, S. R.; Gioia L. D.; Zampella, G.; Diiron dithiolato carbonyls related to the H_{ox}^{CO} state of [FeFe]-hydrogenase. J. Am. Chem. Soc., 2008, 130, 5293-5301.

(36) Ghosh, S.; Hogarth, G.; Hollingsworth, N.; Holt, K. B.; Kabirc, S. E.; Sancheza, B. E. Hydrogenase biomimetics: $Fe_2(CO)_4$(μ-dppf)(μ-pdt) (dppf=1,1'-bis(diphenylphosphino)ferrocene) both a proton-reduction and hydrogen oxidation catalyst. Chem. Commun., 2014, 50, 945-947.